archives
of thermodynamics
Vol. **33**(2012), No. 1, 123–137
DOI: 10.2478/v10173-012-0006-z

Chaotic air pressure fluctuations during departure of air bubbles from two neighbouring nozzles

ROMUALD MOSDORF*
TOMASZ WYSZKOWSKI

Bialystok University of Technology, Faculty of Mechanical Engineering,
Wiejska 45C, 15-351 Białystok

Abstract In the experiment, bubbles were generated from two brass nozzles with inner diameters of 1.1 mm. They were submerged in the glass tank filled with distilled water. There have been measured the air pressure fluctuations and the signal from the laser-phototransistor sensor. For analysis of the pressure signal the correlation (the normalized cross – correlation exponent) and non-linear analyses have been used. It has been shown that hydrodynamic interactions between bubbles can lead to bubble departure synchronization. In this case the bubble departures become periodic. The results of calculation of correlation dimension and the largest Lyapunov exponent confirm that hydrodynamic bubble interactions observed for 4 mm spacing between nozzels cause the periodic bubble departures from two neighbouring nozzles.

Keywords: Bubble chain; Bubble dynamics; Chaotic dynamics

Nomenclature

C	–	correlation coefficient
C_a	–	autocorrelation function
C^2	–	correlation integral
d	–	distance in phase space
D	–	bubble departure diameter
D_2	–	correlation dimension
f	–	frequency of bubble departures, Hz

*Corresponding author. E-mail address: r.mosdorf@pb.edu.pl

H – Heaviside's step function
L – largest Lyapunov exponent
m – number of examined points
N – number of samples
p – probability
q – air volume flow rate, dm^3/min
S – spacing between nozzles, mm
t – time, s
x – sample value

Greek symbols

τ – time delay (number of samples)
σ – standard deviation

Subscripts

a – autocorrelation function
i – sample number
L – left
n – sample number
R – right
p – pressure

1 Introduction

There are numerous physical parameters such as: physical properties of two phases, gas flow rate, gas pressure, height of the liquid and gravity conditions which influence the bubble formation. When bubbles are generated from many nozzles or orifices the complex interactions between them appear. Bubble interactions including its coalescence change the mean size of bubbles and liquid flow around them, and finally the efficiency of the gas-liquid mass transfer processes [1]. Therefore, bubble interactions are still analysed [2,3].

There are numerous papers describing the chaotic behaviours in the bubbling process. In the paper [4] it has been shown that interaction between bubbles in the vertical column causes the chaotic changes of volume fraction of the fluid. The chaotic bubble behaviours are connected with flow instabilities caused by bubble interactions [5] or coalescence between bubbles [6]. The period-doubling sequence of time between bubbles which is leading to chaos has been described in [7]. The tripled period has also been observed [8]. It has been shown that for different nozzle diameters the chaos appears in different ways [9]. It was found that the meniscus oscillations in the orifice strongly affect the subsequent bubble cycle [10,11]. The chaotic behaviours of bubble departures have also been discussed in papers [12–14].

In the papers [15,16] the paths of bubbles emitted from the brass nozzle have been analysed. It has been shown that bubble paths have multifractal character and its properties are changed when bubble departure frequency is greater than 30 Hz.

When the bubbles are generated from two neighbouring nozzles or orifices then hydrodynamic interactions and coalescence between bubbles cause increasing of the chaotic bubble behaviours. In the paper [2] there has been analyzed the interaction between bubbles generated from two adjacent micro-tubes. The analysis shows that the coalescence time depends on the liquid properties, the distance between tubes and the gas flow rate. In the work [3], the coalescence rate of bubbles generated from two separated orifices has been studied and modelled. The coalescence has been analyzed from mechanistic and statistical approach.

In the present paper bubbles were generated from two brass nozzles with inner diameters of 1.1 mm. They were submerged in the glass tank filled with distilled water. There has been analyzed the bubble departures and interactions occurring for different distances between the nozzles and different air volume flow rates. There has been measured the air pressure and signal from the laser-phototransistor sensor. For analysis of the pressure signal the correlation and non-linear methods (correlation coefficient, attractor reconstruction, largest Lyapunov exponent and correlation dimension) have been used.

2 Experimental setup and data recording methods

In the experiment bubbles were generated from two brass nozzles – each of them had inner diameter of 1.1 mm and was located in the tank (400× 400×700 mm) filled with distilled water. The mean bubble departure diameter was about 5.8 mm for frequency of bubble departures equal to 36 Hz. The distance between nozzles was changed from 2 mm up to 10 mm. The distance between nozzles was measured as the spacing between centres of the nozzles.

The gas pressure fluctuations have been measured using uncompensated silicon pressure sensor MPX12DP. For synchronization of pressure signal with bubble location the laser-phototransistor system has been used. In this system the semiconductor red laser with wave length of 650 nm, 3 mW, special aperture and phototransistor BPYP22 have been used. The diameter of laser beam was ∼0.2 mm. The water temperature was 20 °C. The air

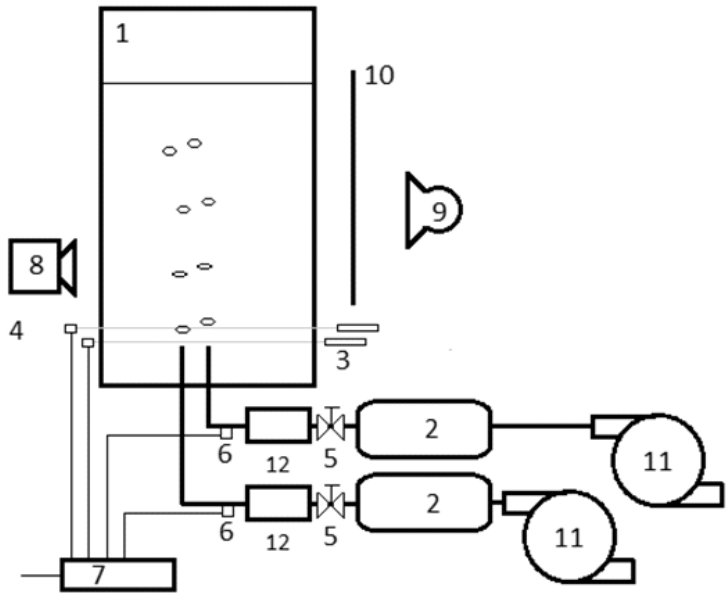

Figure 1. Experimental setup. 1 – glass tank, 2 – air tank, 3 – laser, 4 – phototransistor, 5 – air valve, 6 – pressure sensor, 7 – computer aided data acquisition system, 8 – high speed digital camera, 9 – light source, 10 – screen, 11 – air pump, 12 – flow meter.

volume flow rate was measured using the flow meter (KYTOLA OY, A-2k) and was changed from 0.05 dm^3/min to 0.3 dm^3/min.

The pressure and signal from phototransistor were simultaneously recorded using data acquisition system DT9800 series USB Function Modules for Data Acquisition Systems with sampling frequency of 2000 Hz. The samples were recorded during the 60 s for each air volume flow rates. Each of nozzles had the own air supply system, consisting of 2 dm^3 capacity air tank, flow meter and the air pump. In the experiment the air volume flow rates in both nozzles was the same. The scheme of experimental stand is shown in Fig. 1. Bubble departures have been recorded using the high speed Casio EX FX1 camera. In Fig. 2 it is shown the example of data recorded in the experiment. The signals recorded by pressure sensor and laser-phototransistor are shown. The bubble location over the nozzle is schematically shown over the chart. When the bubble was passing through the laser beam (passing about 3 mm above the nozzle outlet) the phototransistor sensor generated the signal of the low voltage level. During this

time the bubble growth and air pressure in the air supply system decreases. Following the bubble departure, the air pressure increases.

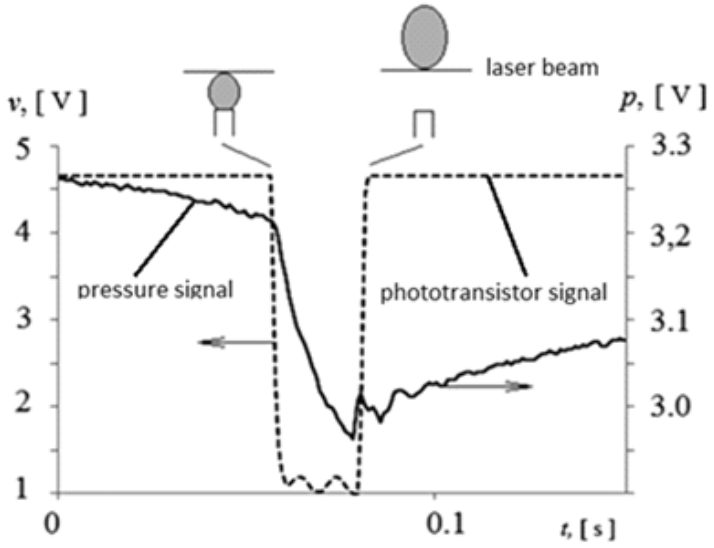

Figure 2. Example of pressure and phototransistor signals.

The number of minima of pressure signal and number of periods with low voltage level signal from phototransistor sensor have been used to determine bubble departure frequencies. In Fig. 3 there is shown the example of frequencies of bubble departures as the function of the air volume flow rate and spacing between nozzles. Interactions between bubbles departing from two neighbouring nozzles cause the significant decreasing the bubble departures frequency (Fig. 3 for the distance between nozzles is equal to 4 mm). When this distance increases to 10 mm (Fig. 3 for $S = 10$ mm), then interactions between bubbles do not change the mean frequency of bubble departures.

3 Bubble behaviours

The examples of bubble behaviours recorded during the experiment are shown in Fig. 4.

In case of the single nozzle, for the air volume flow rate less than 0.2 dm^3/min (Fig. 4a) the air pressure fluctuations do not cause the signif-

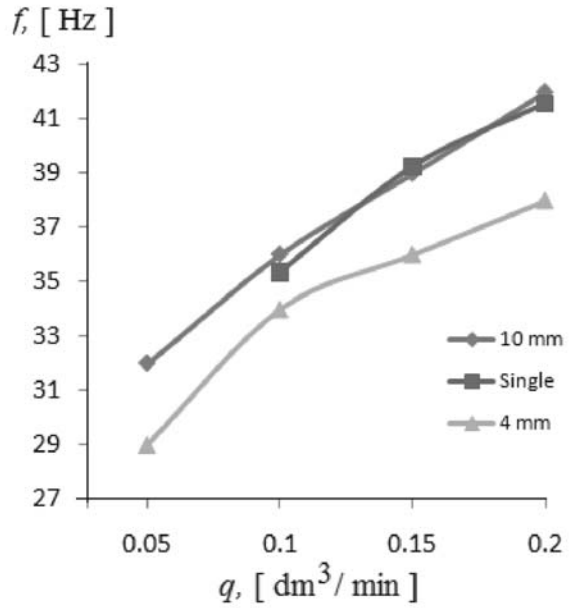

Figure 3. Bubble departure frequency of from the single nozzle and two nozzles with different spacing between them.

icant changes of bubble departure frequencies. The chaotic pressure fluctuations are accompanied by small chaotic changes of frequency of bubble departures less than 4%. When the air volume flow rate increases above 0.2 dm^3/min (Fig. 4c), the interactions between departing bubbles cause the appearance of chaotic changes of bubble departure frequency.

In case of two neighbouring nozzles the vertical, horizontal and declining hydrodynamic interactions and coalescence are observed depending on the spacing between nozzles and air volume flow rate. These interactions can enhance chaotic bubble behaviours (Fig. 4f) or introduce the order in bubble flow over the nozzle outlets (Figs. 4d, e). In the second case the synchronization of bubble departures is observed.

For the spacing between nozzles equal to or greater than 8 mm ($S/D = 1.4$) and volume flow rate $q < 0.1$ dm^3/min the bubble chains over each of nozzles are similar to the bubble chain occurring over the single nozzle. Bubbles form over each of nozzles the separated bubble chains with separated bubbles. When the air volume flow rate increases ($q > 0.1$ dm^3/min, for the spacing between nozzles equal to or greater than 8 mm) then the

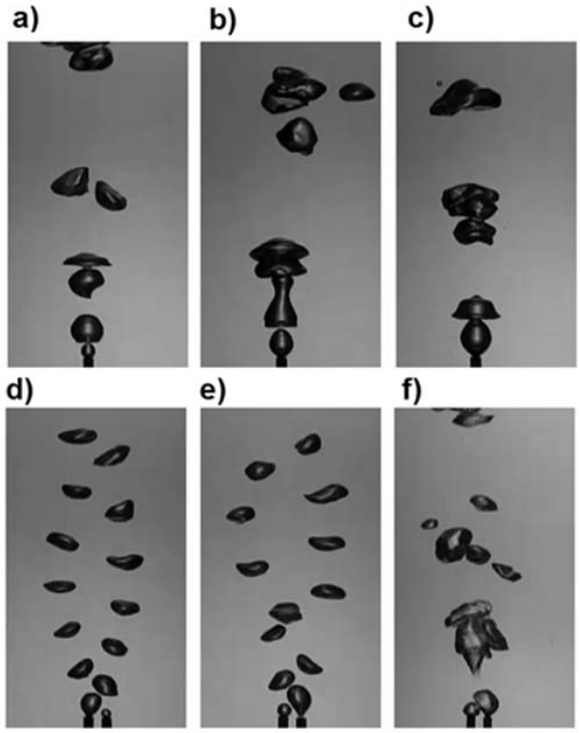

Figure 4. The typical bubble behaviours for bubble chain formation from the single nozzle and two neighbouring nozzles for different air volume flow rates and $S = 4$ mm: a) single nozzle, $q = 0.15$ dm^3/min; b) single nozzle, $q = 0.2$ dm^3/min; c) single nozzle, $q = 0.3$ dm^3/min; d) two neighbouring nozzles; $q = 0.15$ dm^3/min; e) two neighbouring nozzles, $q = 0.2$ dm^3/min, f) two neighbouring nozzles, $q = 0.3$ dm^3/min.

bubbles start to group or coalesce vertically in the vicinity of the nozzle outlets. It causes that the bubble chains become unstable and trajectories of bubbles departing from different nozzles start to cross. When the spacing between nozzles is less than 8 mm then bubbles departing from neighbouring nozzles interact: they bounce, coalesce horizontally and declining which causes the destabilization of bubble chains. For spacing between nozzles equal to 4 mm ($S/D = 0.67$) and $q = 0.15$ dm^3/min the hydrodynamic interaction between bubbles cause that the bubbles in chains do not group The mechanism of bubble interactions is shown in Fig. 5 where subsequent frames of high speed video are presented.

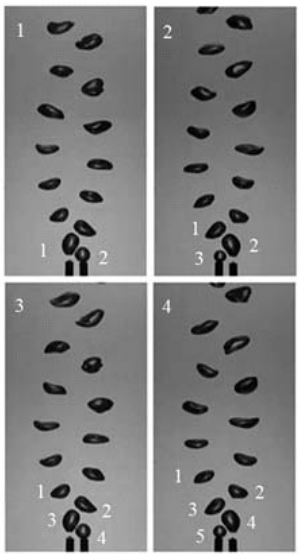

Figure 5. The mechanism of bubble interactions with negative correlation coefficient for $q = 0.15$ dm^3/min and $S = 4$ mm. Time between the frames is equal to 0.015 s.

The time between frames is equal to 0.015 s. The numbers shown in frames identify the subsequent departing bubbles. At first, the bubble '1' attracts the bubble '2'. Then, the bubble '2' is hit by the growing bubble '3', which causes that the bubble '2' starts to move to the right side of the nozzles. Finally, the bubbles in chains are being separated, and then the bubble chains repeal.

4 Correlation analysis

The correlation coefficient between air pressure fluctuations in nozzles has been calculated according to the following formula [17]:

$$C_{L,R} = \frac{\mathrm{cov}\left(p_{i,L}, p_{i,R}\right)}{\sigma_{p_{i,L}} \sigma_{p_{i,R}}} \,, \tag{1}$$

where $p_{i,L}$, $p_{i,R}$ are the time series recorded in the left and right nozzles; $\sigma_{p_{i,L}}$, $\sigma_{p_{i,R}}$ are the standard deviations of time series $p_{i,L}$ and $p_{i,R}$, i is a sample number, cov is a covariance function. When $|C_{L,R}|$ is close to 1, time series $p_{i,L}$, $p_{i,R}$ are correlated, but when $|C_{L,R}|$ is close to zero, then the time series $p_{i,L}$, $p_{i,R}$ are not correlated. When the large values in both

series appear at the same time, then $C_{L,R} > 0$; but when large values in first series meet low values in other series, then $C_{L,R} < 0$.

In Fig. 6 the 3D map of correlation coefficient as a function of the spacing between nozzles and air volume flow rate is presented.

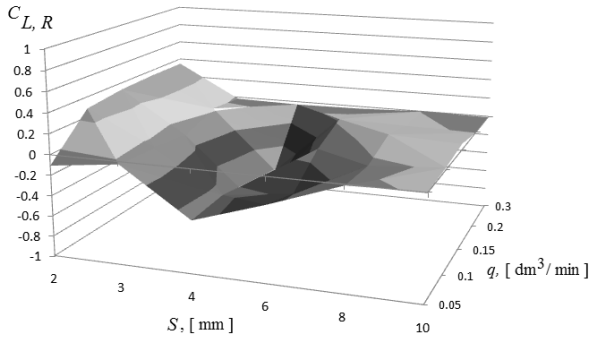

Figure 6. Correlation coefficient of pressure fluctuations for different distances between nozzles and different air volume flow rates.

When the correlation coefficient is positive then the large number of bubbles depart from neighbouring nozzles at the same time. This behaviour is connected with horizontal coalescence of bubbles. When the correlation coefficient is negative then the bubbles depart from nozzles in a way which is shown in Fig. 5. This behaviour is connected with declining interaction between the bubbles. When the correlation coefficient is close to zero the bubble departures from two neighbouring nozzles are independent.

5 Non-linear analysis and discussion

To identify the character of irregular changes of air pressure the non-linear analysis has been performed. The trajectories of the chaotic system in the phase space do not form any single geometrical objects, such as circle or torus, but they form the objects called strange attractors with the structure resembling a fractal [18]. Non-linear analysis starts from attractor reconstruction. In certain embedding dimension reconstruction is carried out using the stroboscope coordination. In this method subsequent coordinates of attractor points are calculated basing on the samples between which the distance is equal to time delay. The time delay is a multiplication of time between the subsequent samples. The image of the attractor in the

n-dimensional space depends upon the time delay. There are many methods which allow to set a proper value of time delay. One of them is based on the analysis of autocorrelation function, C_a. In this case it is assumed that the proper value of time delay, τ obeys the following equation [18]:

$$C_a(\tau) \approx \frac{1}{2} C_a(0) \ . \tag{2}$$

Autocorrelation function enables us to identify the correlation between subsequent samples. The function is defined as follows [18]:

$$C_a(\tau) = \frac{1}{N} \sum_{i=0}^{N} x_i x_{i+\tau} \ , \tag{3}$$

where: N – number of samples, x_i – value of i sample. The function (3) is constant or oscillates when τ increases in case when data is generated by the periodical system [18]. In case of chaotic data the value of autocorrelation function rapidly decreases when τ increases.

In Fig. 7 there have been shown the examples of 3D attractor reconstruction from pressure fluctuations for different air volume flow rates and different distances between nozzles. For $S = 10$ mm and low frequency of bubble departures the pressure fluctuations create the attractor which is characteristic for periodic system (Fig. 7a). The attractor consists of the number of trajectory loops. The shape of the trajectory loop is similar to quadrilateral. When the frequency of bubble departures increases, the amplitude of pressure fluctuations decreases. Therefore, the fluctuations which appear just after bubble departure start to play the important role in shaping the attractor. Changes of the location of 'corners' of attractor in subsequent trajectory loops become larger in comparison with the size of the attractor. The attractor becomes characteristic for deterministic chaos system (Fig. 7d). For $S = 4$ mm and $q = 0.05$ dm^3/min two characteristic time periods between departing bubbles appear. Such behaviour is responsible for the appearance of two loops of attractor trajectory (Fig. 7a, b). The appearance of two loops of attractor trajectory is caused by interactions between bubbles departing from two neighbouring nozzles. Bubbles interactions occurring for $S = 4$ mm cause that structure of attractors for $q > 0.1$ dm^3/min is simpler than in case when $S = 10$ mm. (Fig. 7c, d).

The correlation dimension D_2 is one of the characteristics of attractors, it allows us to identify the structure of attractors. It is defined by the

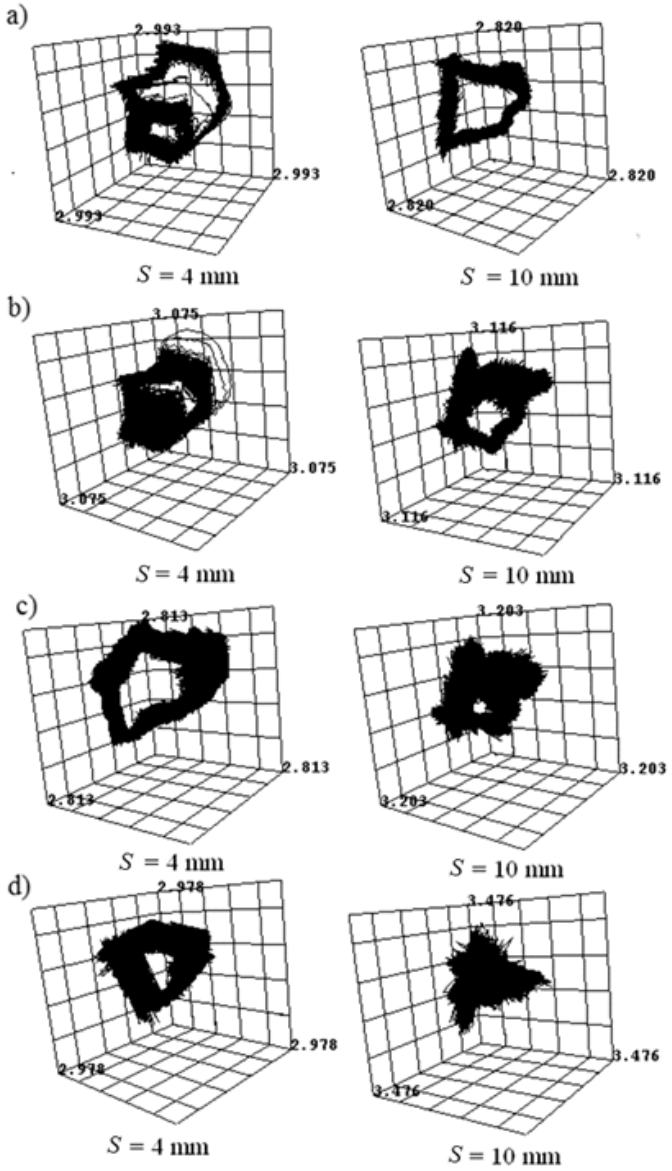

Figure 7. 3D attractor reconstructions for two air volume flow rates and different distances between nozzles: a) $q = 0.05$ dm^3/min, b) $q = 0.1$ dm^3/min, c) $q = 0.15$ dm^3/min, d) $q = 0.2$ dm^3/min.

following expression [18]:

$$D_2 = \lim_{d \to 0} \frac{1}{\ln d} \ln C^2(d) \ , \tag{4}$$

where

$$C^2(d) = \left[\frac{1}{N} \sum_i \left(\frac{1}{N} \sum_j \Theta \left(d - |x_i - x_j| \right) \right) \right] \ , \tag{5}$$

and Θ is the Heaviside's step function that determines the number of attractor's point pairs of the distance shorter than d. The correlation dimension allows us to estimate the number of independent variables describing the system. This number is estimated as the lowest integer number greater than correlation dimension.

The another important characteristics of attractors is the largest Lyapunov exponent. In this case two points on the attractor immersed in M dimensional space have been selected. The distance between these points $d(x_j)$ is at least the one orbiting period. After the lapse of some evolution time the distance of the selected points has been calculated again and denoted as $d(x_{j+1})$. The largest Lyapunov exponent has been calculated according to formula [19]:

$$L = \frac{1}{t} \sum_{j=1}^{m} \log_2 \frac{d(x_{j+1})}{d(x_j)} \ , \tag{6}$$

where m is the number of examined points and t is the time of evolution.

Figure 8 shows results of calculation of correlation dimension and largest Lyapunov exponent of pressure fluctuations for different spacing between nozzles and different air volume flow rates. The obtained results confirm that hydrodynamic bubble interactions observed for $S = 4$ mm cause that bubble departures from two neighbouring nozzles become less chaotic in comparison with bubble departures from single nozzle.

6 Conclusions

In the present paper the chaotic air pressure fluctuations during air bubble departures from two neighbouring nozzles have been investigated.

The calculation of correlation coefficient between air pressure fluctuations in neighbouring nozzles allows us to distinguish two kinds of interactions characterized by positive or negative correlation coefficient. The

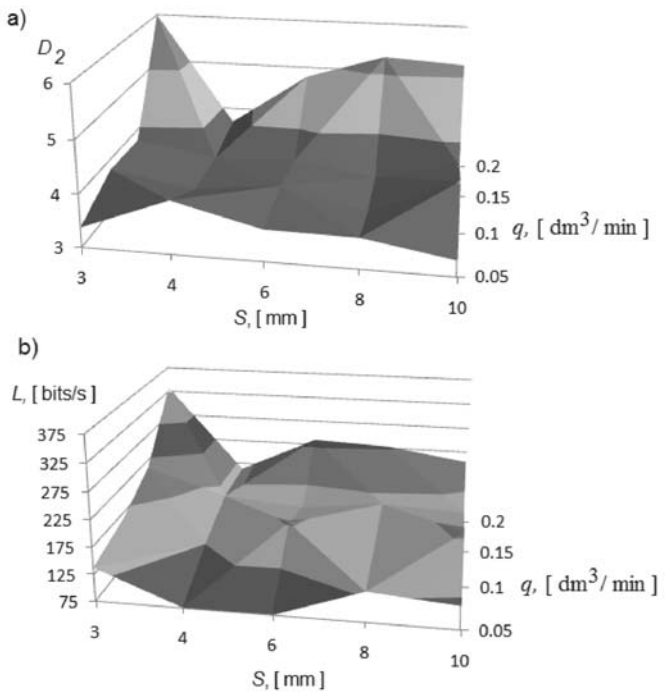

Figure 8. The correlation dimension and largest Lyapunov exponent of air pressure fluctuations for different distance between nozzles and different air volume flow rates: a) correlation dimension, b) largest Lyapunov exponent.

negative correlation is observed when declining bubble interactions appear. It has been shown that such interaction prevents bubbles from coalescence and makes the bubble departures less chaotic in comparison with bubble departures from the single nozzle. This interaction is responsible for the formation of the structure of bubble departures in alternative turns. The results of calculation of correlation dimension and the largest Lyapunov exponent confirm that hydrodynamic bubble interactions observed for $S = 4$ mm cause the periodic bubble departures from two neighbouring nozzles.

When the pattern of bubble flow over the nozzle outlet is stable, then the vertical liquid velocity does not change significantly. In this case subsequent departing bubbles accelerate the liquid flow. The vertical liquid velocity decreases the liquid pressure over the nozzle, and therefore the waiting time decreases. This process causes the decreasing the frequency of bubble departures.

Acknowlegment The authors are grateful for the financial support of Ministry of Science and Higher Education in Poland (Grant: N N503 138936).

Received 4 January 2011

References

[1] Martin M., Garcia J.M., Montes F.J., Galan M.A.: *On the effect of the orifice configuration on the coalescence of growing bubbles.* Chemical Engineering and Processing **47**(2008), 9-10, 1799–1809.

[2] Kazakis N.A., Mouza A.A., Paras S.V.: *Coalescence during bubble formation at two neighbouring pores: An experimental study in microscopic scale.* Chemical Engineering Science **63**(2008), 21, 5160–5178.

[3] Martín M., Montes F.J., Galan M.A.: *Bubble coalescence at sieve plates: II. Effect of coalescence on mass transfer. Superficial area versus bubble oscillations.* Chemical Engineering Science **62**(2007), 6, 1741–1752.

[4] Cieslinski J.T., Mosdorf R.: *Gas bubble dynamics experiment and fractal analysis.* Int. J. Heat and Mass Transfer **48**(2005), 9, 1808–1818.

[5] Femat R., Ramirez J.A., Soria A.: *Chaotic flow structure in a vertical bubble column.* Physics Letters A **248**(1998), 1, 67–79.

[6] Nguyen K., et al.: *Spatio-temporal dynamics in a train of rising bubbles.* The Chemical Engng J. **65**(1998), (1996), 1, 191–197.

[7] Li H.Z., et al.: *Chaotic bubble coalescence in non-Newtonian fluids.* Int. J. Multiphase Flow **23**(1997), 4, 713–723.

[8] Tritton D.J., Egdell C.: *Chaotic bubbling.* Phys. Fluids A **5**(1993), 2, 503–505.

[9] Zhang L., Shoji M.: *Aperiodic bubble formation from submerged orifice.* Chemical Engineering Science **56**(2001), 18, 5371–5381.

[10] Ruzicka M.C., Bunganic R., Drahoš J.: *Meniscus dynamics in bubble formation. Part I: Experiment.* Chemical Engineering Research and Design **87**(2009), 10, 1349–1356.

[11] Ruzicka M.C., Bunganic R., Drahoš J.: *Meniscus dynamics in bubble formation. Part II: Model.* Chemical Engineering Research and Design **87**(2009), 10, 1357–1365.

[12] Vazquez A., Manasseh R., Sánchez R.M., Metcalfe G.: *Experimental comparison between acoustic and pressure signals from a bubbling flow.* Chemical Engineering Science **63**(2008), 24, 5860–5869.

[13] Ruzicka M.C., et al.: *Intermittent transition from bubbling to jetting regime in gas-liquid two phase flows.* Int. J. Multiphase Flow **23**(1997), 4, 671–682.

[14] Mosdorf R., Shoji M.: *Chaos in bubbling – nonlinear analysis and modelling.* Chemical Engineering Science **58**(2003), 17, 3837–3846.

[15] Mosdorf R., Wyszkowski T., Dąbrowski K.K.: *Multifractal properties of large bubble paths in a single bubble column.* Archives of Thermodynamic **32**(2011), 1, 1–18.

[16] Mosdorf R., Wyszkowski T.: *Frequency and non-linear analysis of bubble paths in bubble chain.* Acta Mechanica et Automatica **4**(2010), 1, 72–80.

[17] Gajek L., Kaluszka M.: *Statistics, models and methods.* WNT Warsaw 2000 (in Polish).

[18] Schuster H.G.: *Deterministic Chaos. An Introduction*, PWN, Warszawa 1993 (in Polish).

[19] Wolf A., Swift J.B., Swinney H.L., Vastano J.A.: *Determining Lyapunov Exponent from a Time series.* Physica D **16**(1985), 3, 285–317.